

SATURATION IN TWO-HARD-SCALE PROCESSES
AT HADRON COLLIDERS

CYRILLE MARQUET

Service de Physique Theorique, CEA/Saclay
91191 Gif-sur-Yvette cedex, France
E-mail: marquet@spht.saclay.cea.fr

A study of saturation effects in two-hard-scale hadronic processes such as Mueller-Navelet jets is presented. The cross-sections are expressed in the dipole framework while saturation is implemented via an extension of the Golec-Biat and Wustho model. The transition to saturation is found to be more abrupt than in cross-sections. Observables with a potentially clear saturation signal are proposed.

1 Introduction

Hard processes involving two perturbative scales lead to cross-sections whose linear high-energy behavior is described by the well-known Balitsky-Fadin-Kuraev-Lipatov (BFKL) [1] equation. However, to respect whatever constraints unitarity may impose, it is well-known that the BFKL equation has to be modified beyond some energy limit, in order to describe cross-sections that saturate. Physically, the idea is that the gluon density in the BFKL ladder grows higher as one increases the energy and that eventually recombinations will occur, limiting the number of gluons in the ladder.

Three measurements for studying this behavior can be considered: the total cross-section in e^+e^- scattering [2,3], Mueller-Navelet jets in hadron-hadron collisions [4], and forward jets in deep inelastic scattering [5,6]. The perturbative scales in these processes are set by either the virtualities of the reaction-initiating photons or the transverse momenta of the measured jets. The aim of this work is to describe in a simple way how saturation effects could appear in those processes.

Following the approach of Golec-Biat and Wustho whose saturation model [7] (GBW) for the proton structure functions provides a simple and elegant formulation of the transition to saturation, we will implement saturation effects in the dipole framework [8,9]. The basis of this approach is to consider that the incident particles fluctuate into colorless quark-antiquark pairs (dipoles) which then interact. Saturation will then be modeled through the dipole-dipole scattering.

While such a study has already been done for the σ_{tot} cross-section [10], our work will focus on Mueller-Navelet jets; the extension to the forward-jet case will be straightforward. The key difference between the σ_{tot} and the Mueller-Navelet jet measurements is that the hard probes are no more virtual photons but the real-state jets. The functions expressing the fluctuation of a virtual photon into dipoles are known from QED, but the description of a forward jet in terms of dipoles requires more care. A first part is devoted to this problem and then saturation predictions within the GBW model are presented. Observables to be studied are proposed.

2 Formulation

Mueller-Navelet jets are processes in which a proton strongly interacts with another proton or antiproton and where a jet with transverse momentum larger than a perturbative scale is detected in each of the two forward directions. Such hard processes obey the collinear factorization which allows one to deal only with hard cross-sections. The two cuts on the jets transverse momenta will be denoted Q_1 and Q_2 and taken of the same magnitude in order to suppress the DGLAP evolution in the gluon ladder. The rapidity interval between the two jets is taken to be large in order to lie in the high-energy regime.

Considering first the leading-logarithmic approximation when the evolution is linear, the dipole formulation of this hard total cross-section reads:

$$\sigma(Q_1; Q_2; \dots) = \int d^2 r_1 dz_1 \int d^2 r_2 dz_2 \mathcal{J}(r_1; z_1; Q_1^2) \mathcal{J}(r_2; z_2; Q_2^2) \mathcal{G}_{dd}^{(0)}(r_1; r_2; \dots); \quad (1)$$

where $r_{i=1,2}$ are the transverse sizes of the dipoles interacting and $z_{i=1,2}$ are the fractions of longitudinal momentum of the quarks in each dipole. The BFKL dipole-dipole cross-section is

$$\mathcal{G}_{dd}^{(0)}(r_1; r_2; \dots) = \frac{2}{s} r_1^2 \int_{z_1}^Z \frac{d}{2i} \frac{(r_2=r_1)^2}{(1-y)^2} \exp\left[-\frac{s N_c}{2} (2 - (1-y) - (1+y))\right] \quad (2)$$

where $\psi(x)$ is the logarithmic derivative of the Gamma function. The dipole distributions describing the forward-jet emissions have been denoted $\mathcal{J}(r_i; z_i; Q_i^2)$:

Let us recall how one can obtain this dipole distribution. The k_T -factorization property [1] provides the general formalism for coupling external sources to the BFKL kernel through the convolution of impact factors. It can be proved that k_T -factorization is equivalent [2] to the dipole factorization expressed by formula (1). The dipole distribution \mathcal{J} can thus be derived from the corresponding impact factors: the derivation [3,4,15] is made using the example of a final-state gluon with transverse momentum larger than Q being emitted from a perturbative onium ($q\bar{q}$ state) of size $r_0 = 1 = Q_{CD} : QCD$ factorization will allow to extend the result to the case of an incident hadron since the onium structure function factorizes out. Using k_T -factorization in the BFKL framework, the impact factor $f(k^2; r_0)$ of the onium + jet system is related to the elementary gluon-dipole coupling $f^0(k^2; r)$ in the following way [4,15]:

$$f(k^2; r_0) = \frac{2}{s} \frac{s N_c}{x_J} \log \frac{1}{x_J} \log Q r_0 \int d^2 r \frac{Q}{2-r} J_1(Qr) f^0(k^2; r) \quad (3)$$

in the collinear approximation $Q r_0 = 1$ for the onium. k is the transverse momentum of the gluon connected to the BFKL kernel and x_J is the fraction of longitudinal momentum of the jet with respect to the onium. Formula (3) can be interpreted as the equivalence for forward jets between the momentum-space (partonic) and coordinate-space (dipole) representations. The factor in brackets $f(2/s N_c) \log Q r_0 \log 1/x_J$ corresponds to the probability of finding a dipole of size $l=Q$ inside the onium of size r_0 ; thanks to QCD factorization properties, it is included in the gluon structure function of the incident particle (here the

onium). $f^0(k^2; r) = (1 - J_0(kr)) = k^2$ is nothing else than the gluon density inside the dipole of size r and, in the dipole formulation (1), is included in the dipole-dipole cross-section $\sigma_{dd}^{(0)}$. Having factorized out both the contribution to the structure function F_2 and to the dipole-dipole cross-section, one is left with the function $\int_J(r; Q^2) dz \int_J(r; z; Q^2)$ which describes the resulting size distribution of the interacting dipole. Hence, one is led to identify

$$\int_J(r; Q^2) = \frac{Q}{2r} J_1(Qr) : \tag{4}$$

Let us now consider saturation effects. Initially, the GBW approach [7] is a model for the dipole-proton cross-section which includes the saturation damping of large-dipole configurations. For the description of hard cross-sections at LEP [10], it has been extended to dipole-dipole cross-sections:

$$\sigma_{dd}(r_1; r_2; Q^2) = \sigma_0 \left(1 - \exp\left(-\frac{r_e^2(r_1; r_2)}{4R_0^2(Q^2)}\right) \right) : \tag{5}$$

The dipole-dipole effective radius $r_e^2(r_1; r_2)$ is defined through the two-gluon exchange:

$$2 \int_s \frac{r_e^2(r_1; r_2)}{s} \sigma_{dd}^{(0)}(r_1; r_2; 0) = 2 \int_s \frac{r_e^2(r_1; r_2)}{s} \ln(r_1^2; r_2^2) + 1 + \log \frac{\max(r_1; r_2)}{\min(r_1; r_2)} \tag{6}$$

while for the saturation radius $R_0(Q^2) = e^{-\frac{1}{\Lambda^2} Q^2} = Q_0$ we shall use the same set of parameters as those in [7,10], that is $\sigma_0 = 0.288$; $Q_0 = 8.1$ for $Q_0 = 1$ GeV. Two other scenarios for $r_e^2(r_1; r_2)$ have also been considered: $r_e^2 = r_1^2 r_2^2 = (r_1^2 + r_2^2)$ and $r_e^2 = \min(r_1^2; r_2^2)$:

We shall use σ_{dd} in the hard cross-section (1) instead of $\sigma_{dd}^{(0)}$ to implement saturation in a simple way. However, in order to do so, one makes the non-trivial assumption that the dipole factorization still holds when the dipole-dipole cross-section is modified by saturation.

3 Phenomenology

Inserting (4) and (5) in formula (1) leads to the simple final result for the Mueller-Navelet hard cross-sections modified by saturation within the GBW model:

$$\sigma(Q_1; Q_2; Q^2) = \sigma_0 = 1 - 2R_0^2(Q_1; Q_2) \int_0^1 du \frac{e^{-(Q_1^2 + Q_2^2 u^2) R_0^2 = r_{eff}^2(1; u)}}{r_e^2(1; u)} I_1 \frac{2Q_1 Q_2 u R_0^2}{r_e^2(1; u)} : \tag{7}$$

Some comments are in order. The dipole distribution $\int_J(r; Q^2)$ is not everywhere positive and we interpret this feature as a breakdown of the collinear approximation. It also means that one has to check that replacing $\sigma_{dd}^{(0)}$ by σ_{dd} in (1) does not alter the positivity of the hard cross-sections, and this is indeed the case. Another check that our approximations require is that the cross-sections $\sigma_{dd} \xrightarrow{Q \rightarrow \infty} 4R_0^2(Q^2)$; corresponding to the limit of small dipole sizes in (5), lead to hard cross-sections behaving like $1 = R_0^2(Q^2) \max(Q_1^2; Q_2^2)$; as expected from transparency. The model

$r_e^2 = m$ in $(r_1^2; r_2^2)$ does not and therefore we cannot consider it in our approximations.

Let us investigate the phenomenological outcome, for hadron colliders, of our extension of the GBW models to Mueller-Navelet jets. The theoretical hard cross-sections are obtained from formula (7) in terms of the physical variables Q_1, Q_2 and Δ . When plotting them, one observes the expected trend of the GBW model, that is a convergence of the cross-sections towards the full saturation limit $\Delta \rightarrow 0$: In order to appreciate more quantitatively the influence of saturation, it is most convenient to consider the quantities $R_{i=j}$ defined as

$$R_{i=j} = \frac{\sigma(Q_1; Q_2; \Delta_i)}{\sigma(Q_1; Q_2; \Delta_j)}; \quad (8)$$

i.e. the cross-section ratios for two different values of the rapidity interval. These ratios display in a clear way the saturation effects. They also correspond to possible experimental observables since they can be obtained from measurements at fixed values of the jets longitudinal momenta x_{J_1} and x_{J_2} and thus are independent of the structure functions $f(x_{J_i}; Q_i^2)$ of the incident hadrons. Indeed, the experimental measurement is

$$\frac{d^{pp \rightarrow jj+X}_{\text{tot}}}{dx_{J_1} dx_{J_2}} = f(x_{J_1}; Q_1^2) f(x_{J_2}; Q_2^2) \sigma(Q_1; Q_2; \Delta) \quad (9)$$

and the ratio of these cross-sections gives access to R . Such observables have actually been used for a study of Mueller-Navelet jets for testing BFKL predictions at the Tevatron [16,17].

In Fig.1 we plot the values of $R_{4;6=2;4}$ (resp. $R_{8=4}$) as a function of $Q_1 = Q_2 = Q$: $R_{4;6=2;4}$ is the observable that has been considered for the Tevatron [16,17] while $R_{8=4}$ corresponds to realistic rapidity intervals for the LHC. As expected from the larger rapidity range, the decrease of R between the transparency regime and the saturated one is larger for the LHC than for the Tevatron. The striking feature of Fig.1 is that the effect of saturation appears as a sharp transition for some critical range $Q = R_0$: No saturation effects would correspond to R constant equal to the high Q^2 limit of the plots while the full-saturated limit is $R = 1$: Comparing these ratios for Mueller-Navelet jets to those for the measurement for the same values of the rapidity ranges, one interestingly sees that the transition curve is much smoother, a phenomenon explained by the different structure of the dipole distributions. Indeed the formula to compute the σ_{tot} case is also formula (1) but with of course the well-known photon dipole distributions instead of σ_{tot} : As discussed in [13], the dipole distribution $\sigma_{\text{tot}}(r; Q^2)$ has a tail extending towards large dipole sizes, which are more damped by the saturation corrections. Hence σ_{tot} is more abruptly cut by saturation than the photon dipole distribution. Note that saturation effects in forward-jets [18] can be studied in a straightforward manner using our formalism: it requires to combine (1) with both dipole distributions and σ_{tot} :

The signal displayed in Fig.1 shows a clear transition to saturation, however the values of Q at which it occurs are rather low, probably too low for experimental E_T cuts on jets. An interesting way out of this problem could be that

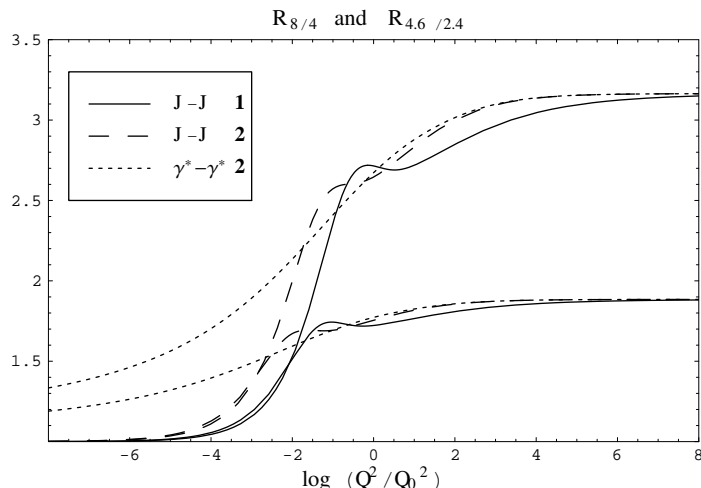


Figure 1. Cross-section ratios $R_{i=j}$: The resulting ratios for the two-gluon exchange model (1) and for $r_e^2 = r_1^2 r_2^2 = (r_1^2 + r_2^2)$ (2) are plotted for rapidity intervals $i=8; j=4$ (highest set of curves) and $i=4; j=2;4$ (lowest set of curves). The comparison is made with ratios for model 2 and equivalent kinematics.

the saturation scale is higher than the one we used in the present work, namely the one extracted from F_2 : Indeed, it has been proposed [19] that the saturation scale could be higher for two-hard-scale processes like Mueller-Navelet jets than for one-hard-scale measurements like the proton structure functions. That would shift the transition shown in Fig.1 towards higher Q : Another alternative to solve this "low- Q " problem would be to consider the detection of heavy vector or heavy-flavored mesons as alternatives to forward jets. Indeed, using J/ψ ; ψ' ; D^0 ; B mesons may provide hard probes of lower transverse momenta than jets, allowing to look deeper in the saturation regime.

These possibilities of realizing hard hadronic probes of saturation certainly deserve more studies in the near future. On the theoretical side, going beyond our approximations seems necessary while on the phenomenological side, simulations at Tevatron and LHC energies will be needed to give a quantitative estimate of the potential of hadronic colliders to reveal those new features of saturation.

Acknowledgements

The author wishes to thank Robi Peschanski for the collaboration. He also thanks Stephane Munier and Christophe Royon for useful comments and suggestions.

References

1. L. N. Lipatov, Sov. J. Nucl. Phys. 23, (1976) 338; E. A. Kuraev, L. N. Lipatov and V. S. Fadin, Sov. Phys. JETP 45, (1977) 199; I. I. Balitsky and

- L. N. Lipatov, *Sov. J. Nucl. Phys.* 28, (1978) 822.
2. J. Bartels, A. De Roeck and H. Lotter, *Phys. Lett. B* 389 (1996) 742; S. J. Brodsky, F. Hautmann and D. E. Soper, *Phys. Rev. D* 56 (1997) 6957.
 3. M. Boonekamp, A. De Roeck, C. Royon and S. Wallon, *Nucl. Phys. B* 555 (1999) 540.
 4. A. H. Mueller and H. Navelet, *Nucl. Phys. B* 282 (1987) 727.
 5. A. H. Mueller, *Nucl. Phys. Proc. Suppl. B* 18C (1990) 125; *J. Phys. G* 17 (1991) 1443.
 6. J. Bartels, A. De Roeck and M. Loewe, *Zeit. für Phys. C* 54 (1992) 635; W.-K. Tang, *Phys. Lett. B* 278 (1992) 363; J. Kwiecinski, A. D. Martin, P. J. Sutton, *Phys. Rev. D* 46 (1992) 921.
 7. K. Golec-Biernat and M. Wustho, *Phys. Rev. D* 59 (1998) 014017, *Phys. Rev. D* 60 (1999) 114023.
 8. N. N. Nikolaev and B. G. Zakharov, *Zeit. für Phys. C* 49 (1991) 607; *Phys. Lett. B* 332 (1994) 184.
 9. A. H. Mueller, *Nucl. Phys. B* 415 (1994) 373; A. H. Mueller and B. Patel, *Nucl. Phys. B* 425 (1994) 471; A. H. Mueller, *Nucl. Phys. B* 437 (1995) 107.
 10. N. Tmneanu, J. Kwiecinski and L. Motyka, *Eur. Phys. J. C* 23 (2002) 513, *Acta Phys. Polon. B* 33 (2002) 1559 and 3045.
 11. S. Catani, M. Ciafaloni and F. Hautmann, *Nucl. Phys. B* 366 (1991) 135. J. C. Collins and R. K. Ellis, *Nucl. Phys. B* 360 (1991) 3; E. M. Levin, M. G. Ryskin, Yu. M. Shabelsky and A. G. Shuvaev, *Sov. J. Nucl. Phys.* 53 (1991) 657.
 12. S. Munier and R. Peschanski, *Nucl. Phys. B* 524 (1998) 377. A. Bialas, H. Navelet and R. Peschanski, *Nucl. Phys. B* 593 (2001) 438.
 13. R. Peschanski, *Mod. Phys. Lett. A* 15 (2000) 1891.
 14. S. Munier, *Phys. Rev. D* 63 (2001) 034015.
 15. C. Marquet and R. Peschanski *Phys. Lett. B* 587 (2004) 201.
 16. D0 Collaboration: B. Abbott, et al, *Phys. Rev. Lett.* 84 (2000) 5722.
 17. J. G. Contreras, R. Peschanski and C. Royon, *Phys. Rev. D* 62 (2000) 034006; R. Peschanski and C. Royon, *Pomeron intercepts at colliders*, Workshop on physics at LHC, hep-ph/0002057.
 18. C. Marquet, R. Peschanski, and C. Royon, to appear.
 19. M. Kozlov and E. Levin, *Eur. Phys. J. C* 28 (2003) 483.